

RESEARCH

Open Access



Changes in albedo and its radiative forcing of grasslands in East Asia drylands

Qingsong Zhu¹, Jiquan Chen², Liangxu Wu¹, Yuting Huang¹, Changliang Shao³, Gang Dong⁴, Zhe Xu¹ and Xianglan Li^{1*} 

Abstract

Background Grasslands in drylands are increasingly influenced by human activities and climate change, leading to alterations in albedo and radiative energy balance among others. Surface biophysical properties and their interactions change greatly following disturbances. However, our understanding of these processes and their climatic impacts remains limited. In this study, we used multi-year observations from satellites and eddy-covariance towers to investigate the response of albedo to variables closely associated with human disturbances, including vegetation greenness (EVI) and surface soil volumetric water content (VWC), as well as snow cover and clearness index (T_a) for their potential relationships.

Results EVI and VWC during the growing season were the primary factors influencing albedo. EVI and VWC were negatively correlated with albedo, with VWC's total direct and indirect impacts being slightly smaller than those of EVI. During the non-growing season, snow cover was the most influential factor on albedo. VWC and T_a negatively affected albedo throughout the year. We estimated the impact of variations in EVI and VWC on climate to be in the range of 0.004 to 0.113 kg CO₂ m⁻² yr⁻¹ in CO₂ equivalent.

Conclusions This study indicates the significant impacts of climate change and human disturbances on vulnerable grassland ecosystems from the perspective of altered albedo. Changes in vegetation greenness and soil properties induced by climate change and human activities may have a substantial impact on albedo, which in turn feedback on climate change, indicating that future climate policies should take this factor into consideration.

Keywords Albedo, Global warming potential, Grassland, Disturbance

Introduction

Among the changes in land surface properties, changes in surface albedo directly influence regional and global climate (Betts 2000; Lee et al. 2011; Carrer et al. 2018; Sciusco et al. 2020, 2022; Abraha et al. 2021; Ouyang et al. 2022; Lei et al. 2023). The magnitude and the spatiotemporal changes of surface albedo, the ratio of reflected to incoming short-wave radiation, represents the amount of radiation leaving the earth system. In turn, this leads to warming or cooling regulations on climate, together with the effects of greenhouse gases (GHGs, e.g., CO₂, CH₄ and N₂O) and atmospheric conditions (e.g., aerosols, clouds) (Forster et al. 2021). In its 6th Assessment Report, the Intergovernmental Panel on Climate Change (IPCC) indicated that albedo-induced radiation forcing

*Correspondence:

Xianglan Li
xlli@bnu.edu.cn

¹ State Key Laboratory of Remote Sensing Science, College of Global Change and Earth System Science, Faculty of Geographical Science, Beijing Normal University, Beijing, China

² Department of Geography, Environment, and Spatial Sciences, Michigan State University, East Lansing, MI 48823, USA

³ State Key Laboratory of Efficient Utilization of Arid and Semi-Arid Arable Land in Northern China, National Hulunber Grassland Ecosystem Observation and Research Station, Institute of Agricultural Resources and Regional Planning, Chinese Academy of Agricultural Sciences, Beijing, China

⁴ School of Life Science, Shanxi University, Taiyuan, China

(RF) was $0.20 \pm 0.10 \text{ W m}^{-2}$, accounting for 9.3% of the total RF attributed to increasing CO_2 concentrations ($2.16 \pm 0.25 \text{ W m}^{-2}$). This may be underestimated compared to other results in the literature (Betts 2000; Lee et al. 2011; Lei et al. 2023).

Dryland regions in Eurasia have experienced rapid changes in ecosystems and associated surface properties due to both the warming climate and socioeconomic development (Groisman et al. 2009; Qi et al. 2017; Chen et al. 2022b). Native grasslands are the dominant ecosystem type in this region. These ecosystems have been extensively converted through agricultural intensification, urbanization, desertification, and overgrazing among other land use changes (John et al. 2009; Chen et al. 2018; Zheng et al. 2019; Venkatesh et al. 2022a, 2022b; Yuan et al. 2022). Tian et al. (2014, 2017) examined the spatial relationships between albedo and vegetation on the Tibetan and Mongolian plateaus and found close spatial coherencies. While other human activities, such as grazing and harvesting, may not cause explicit changes in land cover types, they have been found to significantly influence canopy cover, leaf area, snow cover, and soil moisture, consequently leading to changes in albedo (Dedieu et al. 2014; Zhang et al. 2014; John et al. 2016; Dong et al. 2021; Venkatesh et al. 2022a). As climate change and the coupling between ecosystems and societal systems strengthen, grasslands may face heightened anthropogenic disturbances, further inducing alterations in albedo and feedback on climate. The ecological impacts of disturbances on ecosystems and the potential radiation forcing (RF) induced by albedo changes have long been research foci in dryland regions.

Previous studies have highlighted a broad spatial link between the greening of vegetation and decreased albedo during the growing season due to changes in vegetation structure and further radiative transfer processes based on satellite data (Tian et al. 2014). Through in situ observations, it has been found that albedo of sparsely vegetated surfaces (e.g., grasslands, deserts, and shrublands) is especially susceptible to factors such as soil moisture, snow cover, and atmospheric conditions (Briegleb et al. 1986; Lobell and Asner 2002; Wang et al. 2005; Yang et al. 2014; Li et al. 2019). However, little is known about albedo dynamics in grassland ecosystems that undergo frequent disturbances. These disturbances not only impact above-ground vegetation cover characteristics, such as vegetation structure and biomass, but also affect soil properties. The dynamics of these properties drive changes in albedo. Previous studies using satellite observations often simplified the modelling of albedo changes since they can only observe the land surface over short periods. This approach may overlook other factors influencing albedo and its dynamics. Currently, there is a lack

of detailed investigations and assessments of the various factors influencing albedo in disturbed grassland ecosystems through ground measurements which offer higher spatial and temporal resolutions. Additionally, there is limited research quantifying albedo-induced RF ($\text{RF}_{\Delta\alpha}$) after disturbances, leading to a lack of understanding of the impact of post-disturbance albedo on climate (Betts 2000; Abraha et al. 2021; Chen 2021; Ouyang et al. 2022; Lei et al. 2023).

In this study, we used multi-year in situ observations of albedo, soil moisture, vegetation indices, snow cover, and microclimate measurements (e.g., temperature) from ten grasslands sites that have available datasets in Asian dryland regions. After illustrating the magnitude and dynamics of albedo at these sites, we examined the multiple forcing mechanisms for the growing season (GS) and non-growing season (NGS) through multiple regression analyses and structural equation modelling (SEM) on albedo (α) and albedo-induced global warming impact ($\text{GWI}_{\Delta\alpha}$). We aim to address the following questions: (1) How do canopy cover, soil, and snowfall directly and indirectly affect albedo across seasons? (2) How important is $\text{GWI}_{\Delta\alpha}$ following ecosystem perturbations?

Materials and methods

Study sites

Our study includes ten grassland sites located in an area between 37°N to 48°N and 101°E to 124°E . Eddy-covariance flux measurements were conducted on six sites in China and four in Mongolia (Fig. 1; Table 1). The sites cover a gradient of arid, semi-arid, and alpine climate. Precipitation is low and the annual Palmer Drought Severity Index varies from -3.87 to 0.18 . Temperature, precipitation, radiation, soil volume moisture content, and carbon flux were observed separately during the growing season (April to October) and non-growing season.

Three observation sites were established in 2014 in shrub grassland (MG-SHB), temperate grassland (MG-TPL), and meadow grassland (MG-MDW) locations in Mongolia. The northernmost meadow grassland site is located in Inner Mongolia, China, and is clipped annually at the end of August (HAI-CMDW). A pair of sites are in Jilin, China: one is degraded saline alkali land that has been fenced from grazing (Cha-NENU) since 2000, and the other is harvested at the end of August (Cha-CMDW). A site in Qinghai (CN-HAM) is part of the FLUXNET2015 (<https://fluxnet.org/>), and another in Qinghai (QHB) and the Kherlenbayan Ulaan site (KBU) are part of the AsiaFlux (<http://asiaflux.net/>). The KBU site is fenced grassland. CN-ham is a winter-grazed grassland and QHB is a seasonally grazed grassland. All sites experience seasonal snowfall during the winter.

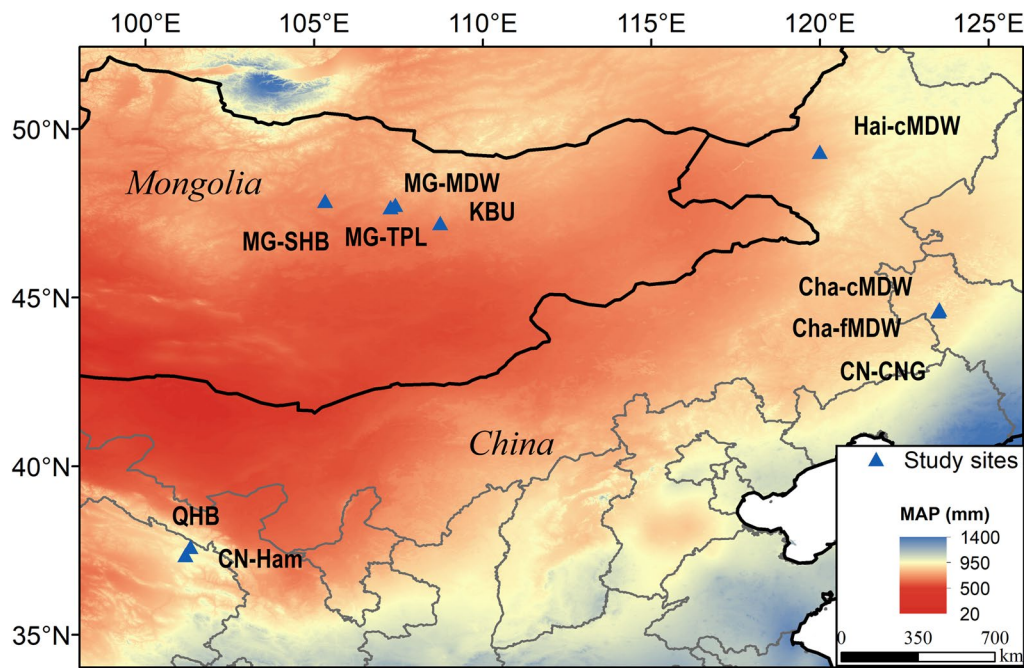


Fig. 1 Location of ten study sites in East Asia (triangles). The coloured background shows the annual average precipitation (MAP) based on the WorldClim Bioclimatic variables V2 dataset (Fick and Hijmans 2017)

Table 1 Location, data spans, and annual Palmer Drought Severity Index (PDSI) of ten eddy-covariance flux sites in Mongolia and China

Site id	Region	Latitude	Longitude	Data span	Altitude (m)	PDSI	References
MG-MDW	Ulaanbaatar, Mongolia	47.75°N	104.71°E	2014–2018	1485	−3.715	Chen et al. (2022a)
MG-SHB	TOV, Mongolia	47.88°N	105.32°E	2014–2018	1281	−2.677	Chen et al. (2022a)
MG-TPL	Ulaanbaatar, Mongolia	47.69°N	107.27°E	2014–2018	1448	−3.788	Chen et al. (2022a)
CHA-NENU	Jilin, China	44.59°N	123.51°E	2018–2021	141	−1.301	Dong et al. (2021)
CHA-CMDW	Jilin, China	44.65°N	123.54°E	2018–2021	139	−1.405	Dong et al. (2021)
HAI-CMDW	Inner Mongolia, China	49.33°N	119.99°E	2018–2021	632	−2.393	Dong et al. (2021)
CN-CNG	Jilin, China	44.59°N	123.51°E	2007–2010	141	−2.781	Dong et al. (2021)
CN-HAM	Qinghai, China	37.37°N	101.18°E	2002–2004	–	0.184	Kato et al. (2006)
KBU	Hentiy, Mongolia	47.21°N	108.74°E	2003–2009	1235	−3.875	Li et al. (2005)
QHB	Qinghai, China	37.61°N	101.33°E	2002–2004	3250	0.639	Cui et al. (2006)

Site-specific data from the eddy flux tower site

On each tower, a four-way radiometer (CNR1 or CNR4) was used to measure incoming and outgoing short- and long-wave radiation (SW_{in} , SW_{out} , LW_{in} and LW_{out} , respectively). Surface albedo (α) was calculated as the ratio of outgoing short-wave radiation to incoming short-wave radiation ($\alpha = SW_{out} / SW_{in}$). We used daytime radiation data between sunrise and sunset to calculate albedo (Chen 2021). Albedo with high solar zenith angle (SZA) ($> 85^\circ$) were discarded. In addition, we included half-hourly air temperature (TA), soil volume moisture content (VWC), and precipitation (P) as

potential drivers on albedo. All data were aggregated to monthly average.

Satellite data

The enhanced vegetation index (EVI) was used as an indicator of vegetation abundance because it reflects many plant properties and activities, such as foliage chlorophyll content, leaf area, and above-ground biomass (Myneni and Williams 1994; Kawamura et al. 2005). EVI has been widely used in grassland studies because it can reduce the influence of soil background and atmospheric aerosol effectively (Huete et al. 2002). We calculated EVI based

on a combination of MODIS reflectance data in the near-infrared, red, and blue spectral bands. The MODIS surface reflectance data were obtained from MODIS Nadir Bidirectional Reflectance Distribution Function-Adjusted Reflectance dataset (MCD43A4 v061, <https://lpdaac.usgs.gov>) which removed view angle effects from the directional reflectance. MCD43A4 v061 product provides daily nadir reflectance and quality label with a 500 m spatial resolution. The data were assessed to match the tower base observation data well (Chu et al. 2021). We used a Savitzky–Golay filter to remove the noise potentially caused by clouds and other atmospheric conditions and reconstruct the time series. We also used MODIS Normalized Difference Snow Index (NDSI) obtained from MODIS Terra Snow Cover product (MOD10A1 v061, <https://lpdaac.usgs.gov>), as an indicator of snow cover. The dataset provides a daily composite of snow cover and basic quality assessment flag with cloud mask, atmospheric correction, and surface temperature screening (Riggs et al. 2017). We considered the data points with an NDSI of >0.1 as snow (Zhang et al. 2019). Depending on the study area, season and validation method, the accuracy of MODIS snow cover products range between 85 and 95% (Coll and Li 2018). Finally, all satellite data were composited to monthly data to match the monthly albedo and meteorological data.

Albedo-induced global warming impact ($\text{GWI}_{\Delta\alpha}$)

Instantaneous short-wave radiation forcing $\text{RF}_{\Delta\alpha}$ at the top of atmosphere was estimated as (Chen 2021; Bright and Lund 2021):

$$\text{RF}_{\Delta\alpha} = -\frac{1}{12} \left(n_{\text{GS}} * \text{SW}_{\downarrow\text{GS}} \cdot \sqrt{T_{a,\text{GS}}} \cdot \Delta\alpha_{\text{GS}} + n_{\text{NGS}} * \text{SW}_{\downarrow\text{NGS}} \cdot \sqrt{T_{a,\text{NGS}}} \cdot \Delta\alpha_{\text{NGS}} \right), \quad (1)$$

where T_a is the atmospheric transmittance of downward short-wave radiation (a.k.a. clearness index), $\Delta\alpha$ is the change of surface albedo, and n is the number of months in the GS or NGS. The two terms represent the actual RF in the growing and non-growing seasons. We used $\sqrt{T_a}$ as an approximation for atmospheric transmittance of upward short-wave radiation (Bright and O'Halloran 2019), where T_a can be calculated as:

$$T_a = \frac{\text{SW}_{\text{in}}}{\text{SW}_{\text{toa}}}, \quad (2)$$

where SW_{toa} is the incident solar radiation at the top of the atmosphere, which is calculated from latitude, longitude, and day of the year (d):

$$\text{SW}_{\text{toa}} = S_{\text{constant}} \cdot \left(1 + 0.344 \cos \left(2d \cdot \frac{\pi}{365.25} \right) \right) \cdot \cos(\psi), \quad (3)$$

where S_{constant} is the solar constant (1367 W m^{-2}).

Finally, we converted $\text{RF}_{\Delta\alpha,\text{GS}}$ due to alteration of albedo in the GS to CO_2 -equivalent ($\text{GWI}_{\Delta\alpha}$) (Carrer et al. 2018; Abraha et al. 2021):

$$\text{GWI}_{\Delta\alpha} = \frac{S \cdot \text{RF}_{\Delta\alpha,\text{GS}}}{\text{AE} \cdot \text{AF}} \cdot \left(\frac{\ln 2 \cdot M_{\text{CO}_2} \cdot m_{\text{air}} \cdot \text{CO}_{2\text{ref}}}{\Delta F_{2x} \cdot M_{\text{air}}} \right) \cdot \frac{1}{\text{TH}}, \quad (4)$$

where $\text{GWI}_{\Delta\alpha}$ is the CO_2 -equivalent from the change of albedo in the GS, S is the perturbed area (1 m^2), AE is the earth's surface area ($5.1 \times 10^{14} \text{ m}^2$), ΔF_{2x} is the radiative forcing per doubling of current CO_2 concentration in the atmosphere (3.7 W m^{-2}), m_{air} is the mass of the atmosphere ($5.148 \times 10^{15} \text{ Mg}$), M_{air} and M_{CO_2} are the molecular weights of air (28.95 g mol^{-1}) and CO_2 (44.01 g mol^{-1}), respectively, $\text{CO}_{2\text{ref}}$ is the reference CO_2 concentration in the atmosphere (389 ppm), TH is the time horizon, set as 100 years following IPCC standards; and AF (i.e. CO_2 airborne fraction) is the percentage of CO_2 emissions left in the atmosphere after a period of time t .

Statistical analysis

We initially estimated the relationships of albedo with the VWC and EVI by using linear, cubic polynomial regression and a mixed effects model with the site as a random effect (Kuznetsova et al. 2017). We analysed the relationship between the EVI and albedo during the GS, whereas the VWC was analysed throughout the year due to its great variations in NGS. As the influence of soil moisture and EVI on albedo may be nonlinear (Sellers 1985; Wang et al. 2005), we used a cubic model to test the non-linear relationship for different variables because it has a flexible form. We also used a linear mixed effects model with site as a random effect, which allowed us to consider the potential differences between sites caused by topography, biomass, and species when fitting the model. We compared the linear model and the cubic model to assess the linearity of the relationships between EVI and albedo, as well as between VWC and albedo. We compared the models using analysis of variance (ANOVA) and Akaike information criterion (AIC). As vegetation dynamics can overshadow the influence of soil moisture during the GS, especially at high canopy cover, we further performed residual analysis to eliminate one variable (i.e. VWC) before exploring the relationship between EVI and albedo. In this analysis, we chose to calculate residuals using the best model selected through model comparison in the previous step. Finally, we examined the relative contributions of the EVI, VWC, and snow

Table 2 Statistical relationship between the monthly albedo, VWC and EVI for the ten sites in growing season

	lm	Poly	lme
Albedo ~ EVI	$r = -0.462; R^2 = 0.213; p < 0.01$ (AIC = -270.9)	$R^2 = 0.251; p < 0.01^*$ (AIC = -279.8)	$R^2 = 0.542; p < 0.01$ (AIC = -375.0)
EVI ~ VWC	$r = 0.303; R^2 = 0.09; p < 0.01$ (AIC = -137.2)	$R^2 = 0.121; p < 0.01^*$ (AIC = -143.1)	$R^2 = 0.755; p < 0.01$ (AIC = -454.2)
Albedo ~ VWC	$r = -0.472; R^2 = 0.223; p < 0.01$ (AIC = -275.6)	$R^2 = 0.259; p < 0.01^*$ (AIC = -282.2)	$R^2 = 0.567; p < 0.01$ (AIC = -384.3)
Albedo ~ [EVI + VWC]	$R^2 = 0.255; p < 0.01$ (AIC = -249.4)	$R^2 = 0.322; p < 0.01^*$ (AIC = -262.9)	$R^2 = 0.602; p < 0.01$ (AIC = -332.0)

The statistics in this study are based on three models: a linear model (lm), a cubic polynomial model (poly), and a linear mixed effects model (lme), with site as a random effect driver to consider site-to-site variability. * Indicates a significant difference between the linear model and polynomial model

through a linear mixed effects model (Table 2). The model was designed as:

$$\text{Albedo} \sim \text{EVI} + \text{VWC} + \text{NDSI} + \text{Ta} + (1|\text{site}), \quad (5)$$

where 1|site was selected as the random effect to account for site as a random, block factor affecting the relationships with EVI, VWC, and NDSI.

We constructed a structure equation model (SEM) to evaluate the complex, interactive relationships between multiple variables and albedo, including direct and indirect impacts. The SEM is a powerful multivariate technique to test multiple possible pathways and to evaluate whether data are consistent with a theoretical, expected initial model (Fan et al. 2016). We conducted the analysis at the annual, growing season, and non-growing season scales. SEMs establish directed paths among different variables to represent causal relationships. Therefore, we employed standardized path coefficients in the SEM to quantify the direct impacts of the EVI and VWC on albedo. Given that the standardized path coefficients in SEMs remove differences in variable scales, we calculated the indirect influence of the VWC on albedo by multiplying the standardized path coefficient between VWC and EVI with the standardized path coefficient between EVI and albedo (i.e. VWC affects albedo by affecting EVI). Finally, the potential impacts of anthropogenic alterations of EVI and VWC on albedo in the growing season were quantified by calculating $\text{GWI}_{\Delta\alpha}$. Specifically, we estimated the potential changes in albedo ($\Delta\alpha$) because of variations in the EVI and VWC during the GS using the regression coefficients of linear regression for corresponding variables. Then, the $\text{GWI}_{\Delta\alpha}$ induced by the indirect impact of EVI and VWC was estimated using methods described in Sect. "Albedo-induced global warming impact". All statistics were conducted in R version 4.2.0.

Results

Seasonal changes in albedo and their drivers

Albedo, vegetation greenness, soil moisture content, and other meteorological variables showed clear seasonal changes as expected (Fig. 2). In general, albedo was low (~0.20) during April–October; while the EVI, temperature, and precipitation were high during July–August. The annual variation of the VWC showed a bimodal distribution while the incoming radiation was high in April/May. The albedo reached 0.78 (HAI-CMDW) in snow-covered months but remained low at 0.26 (QHB) in snowless months. The EVI in the peak GS, mean temperature, precipitation, incoming radiation, and VWC also showed great differences by site and year.

Clipping effects on albedo and radiative forcing

The paired sites with and without clipping treatments provided an opportunity to directly assess the effects of land use on $\text{RF}_{\Delta\alpha}$. Compared with the fenced site (CHA-NENU), the clipped grassland site (CHA-CMDW) had a lower EVI. After reaching a peak in August 2018, CHA-CMDW showed a significantly lower EVI than CHA-NENU (Fig. 3). In 2019, 2020 and 2021, CHA-CMDW had a lower EVI only in July. The maximum difference in the EVI between the two sites was 0.2. CHA-CMDW showed higher VWC (note only two years of data are available). In August 2019, CHA-CMDW had a VWC of 0.38, while CHA-NENU had a VWC of 0.58. The albedo also differed between the two sites, with CHA-NENU having a higher albedo during the GS, while there was no obvious difference during the NGS.

Comparing the albedo at CHA-CMDW with CHA-NENU, we evaluated 3-year $\text{RF}_{\Delta\alpha}$ between clipped and fenced meadow since 2019 (Fig. 4). The difference in albedo yielded a positive $\text{RF}_{\Delta\alpha}$ in the GS (i.e. warming), ranging from 4.6 to 15.9 W m^{-2} . Large variations were found in the NGS, showing a negative $\text{RF}_{\Delta\alpha}$ of -1.6 W m^{-2} in 2019 and -7.2 W m^{-2} in 2020 but a positive $\text{RF}_{\Delta\alpha}$

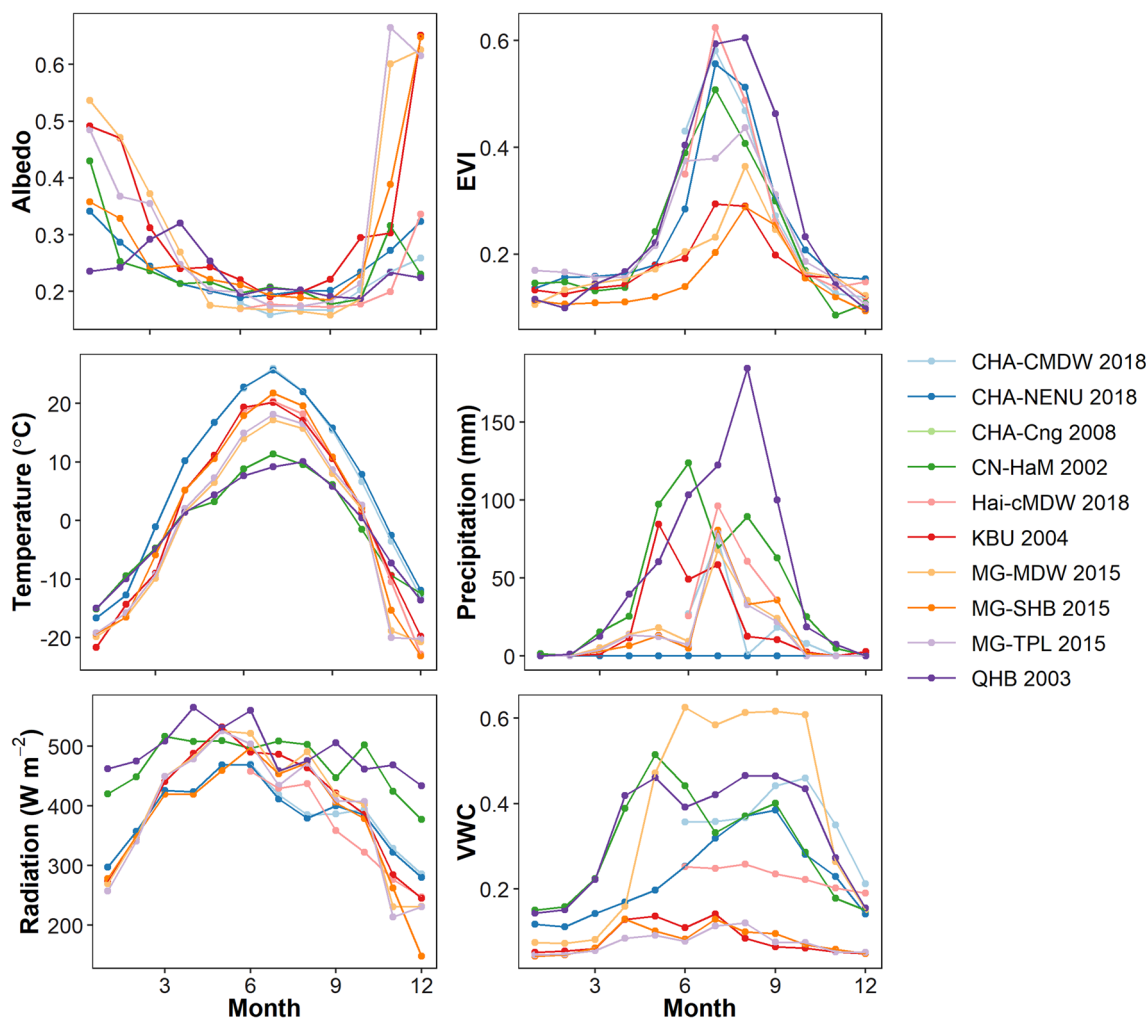


Fig. 2 Seasonal changes in monthly average albedo, enhanced vegetation index (EVI), temperature, precipitation, short-wave radiation, and soil volumetric water content (VWC) at the ten study sites (Fig. 1). The visualization was created using one year of observational data from each site

17.6 W m⁻² in 2021. The annual average $RF_{\Delta\alpha}$ varied from 2.0 to 16.6 W m⁻².

Changes in albedo with vegetation index and soil moisture

Albedo decreased exponentially with EVI and VWC at the ten study sites (Fig. 5). Higher monthly snow-free albedo was observed in the NGS (NDSI=0), ranging from 0.19 to 0.54, while lower values were observed in the GS, with an average of 0.20, albeit with large variations. Compared to the fast decrease during the transition from NGS to GS in response to EVI, albedo responded more slowly to the rising VWC. Interestingly, albedo had a continued decreasing trend even at high soil moisture (VWC>0.60).

VWC was a significant independent variable affecting albedo in both the GS and NGS. However, its

contributions to the variance varied significantly between different model types (Tables 2 and 3). The correlation coefficients between the VWC and albedo were -0.472 and -0.374 in the GS and NGS, respectively. The EVI was also a significant variable on albedo in the growing season ($r = -0.462$). Based on the AIC and R^2 values, the cubic polynomial model outperformed the linear model in both the growing and non-growing seasons. There was a significant positive relationship between the VWC and EVI during the GS. After considering the interactive effects of the EVI and VWC during the GS, the R^2 increased by 0.042 in the linear model while it increased by 0.071 in the polynomial model compared to the model only considering the EVI. The mixed effects accounting for variability between sites, tended to provide a stronger explanatory power compared to linear models.

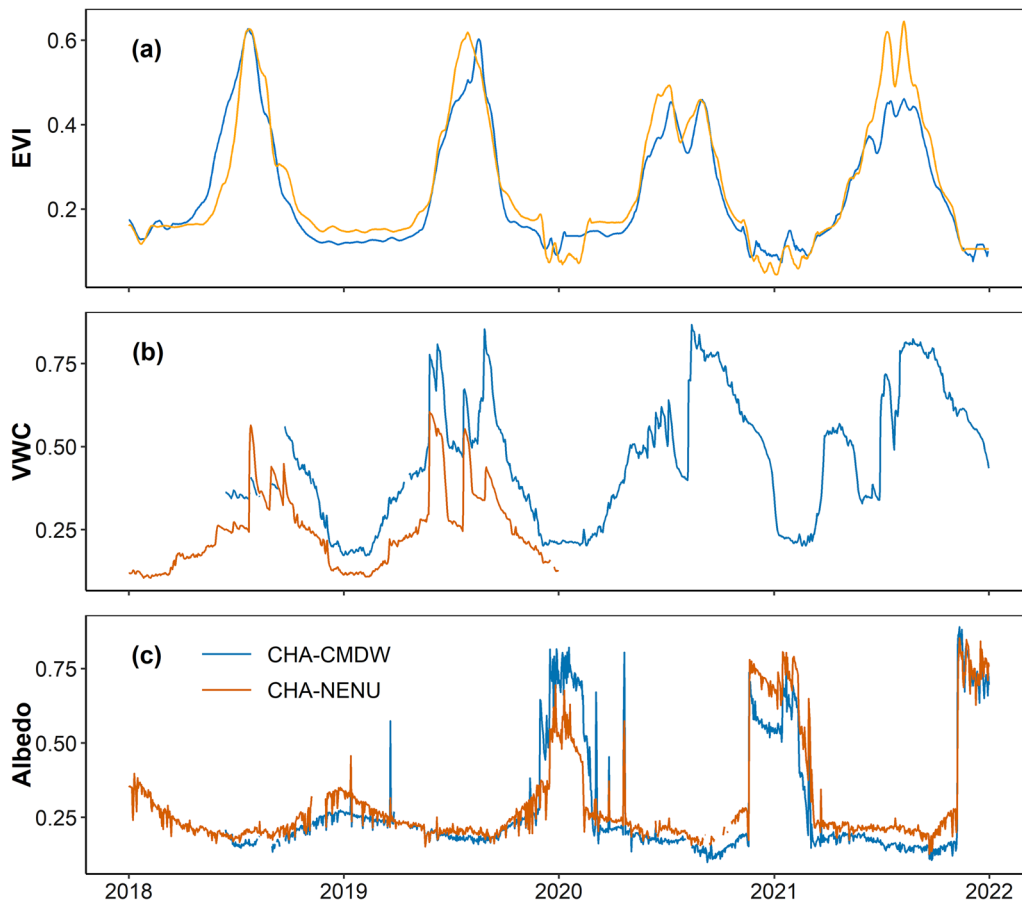


Fig. 3 The average daily enhanced vegetation index (EVI, **a**), volumetric water content (VWC, **b**) and albedo (**c**) in clipped meadow (CHA-CMDW) and fenced meadow (CHA-NENU), showing the consequences of clipping manipulations

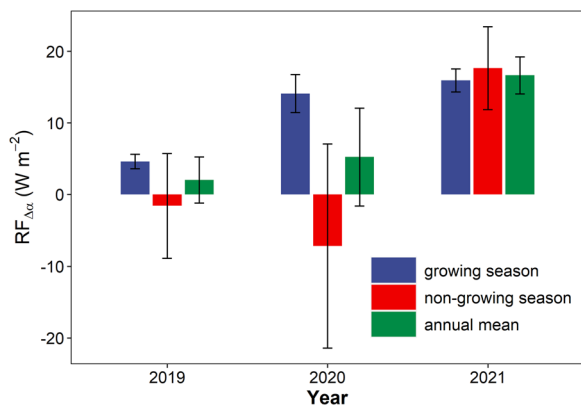


Fig. 4 Average albedo-induced radiative forcing ($RF_{\Delta\alpha}$) due to conversion of fenced meadow (CHA-NENU) to clipped meadow (CHA-CMDW) in the growing season, non-growing season and the annual mean. Error bars indicate the standard errors

After statistically controlling for the impact of VWC on the albedo and EVI (i.e. by regressing on the residuals between VWC and EVI, as well as VWC and albedo), a negative relationship remained between the EVI and albedo in both the growing and non-growing seasons (Fig. 6). The relationship between the EVI and albedo during the non-growing season was notably weak.

Direct and indirect effects of multiple biophysical variables

We designed a similar SEM for the GS, NGS, and year-round by including all potential direct and indirect relationships between albedo and biophysical factors (Fig. 7). All three SEMs showed a non-significant Fisher’s *C* value ($p > 0.05$), indicating that the covariance structure of the model could be accepted. Overall, the EVI, VWC and T_a had significant negative effects on albedo, whereas NDSI

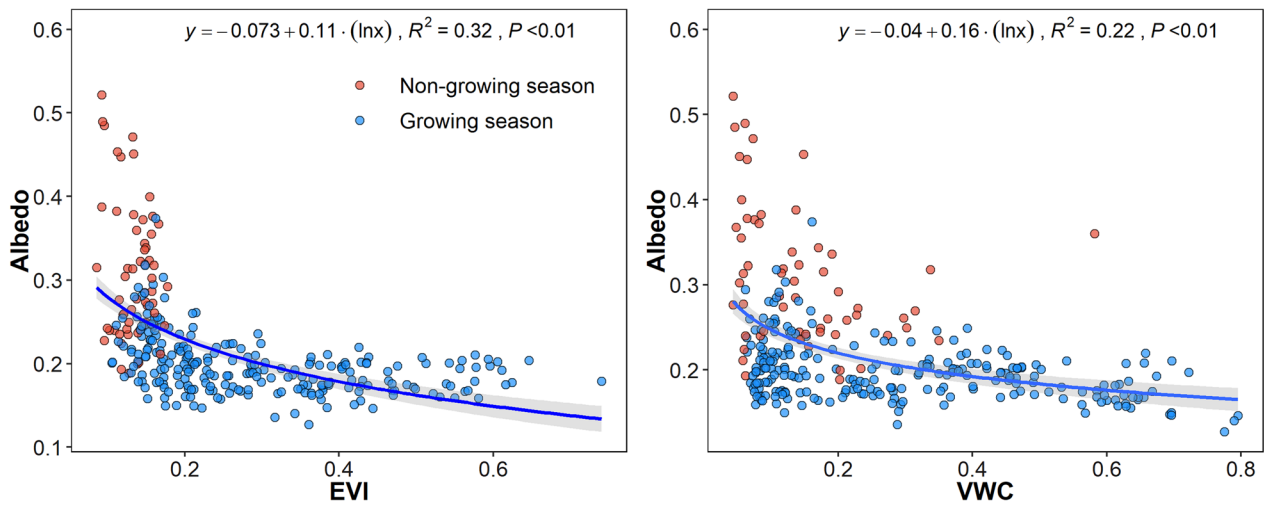


Fig. 5 Changes in monthly mean albedo with EVI and VWC in the growing season and non-growing season at the ten study sites

Table 3 Statistical relationship between the monthly albedo, VWC and EVI for the ten study sites in the non-growing season

	lm	Poly	lme
Albedo ~ EVI	$r = -0.257; R^2 = 0.066; p = 0.06$ (AIC = 151.6)	$R^2 = 0.099; p < 0.01$ (AIC = 149.7)	$R^2 = 0.46; p < 0.01$ (AIC = 106.6)
EVI ~ VWC	NS	NS	NS
Albedo ~ VWC	$r = -0.374; R^2 = 0.14; p < 0.01$ (AIC = 137.9)	$R^2 = 0.230; p < 0.01^*$ (AIC = 123.2)	$R^2 = 0.294; p < 0.01^*$ (AIC = 139.3)
Albedo ~ [EVI + VWC]	$R^2 = 0.184; p < 0.01$ (AIC = 130.9)	$R^2 = 0.289; p < 0.01^*$ (AIC = 116.3)	$R^2 = 0.434; p < 0.01$ (AIC = 110.7)

The statistics are based on three models: a linear model (lm), a cubic polynomial model (poly), and a linear mixed effects model (lme), with site as random effect driver to consider site-to-site variability. *Indicates the significant difference between the linear model and polynomial model, and 'NS' indicates that the regression is not significant

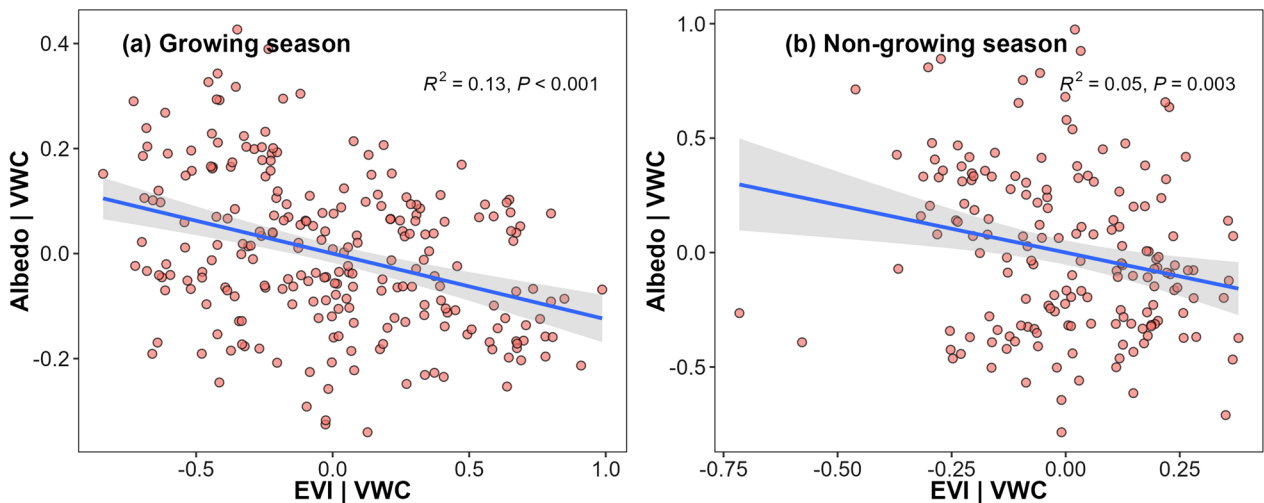


Fig. 6 Partial relationship between residuals of regression for the EVI and VWC and residuals of regression for the albedo and VWC in **a** the growing season and **b** the non-growing season

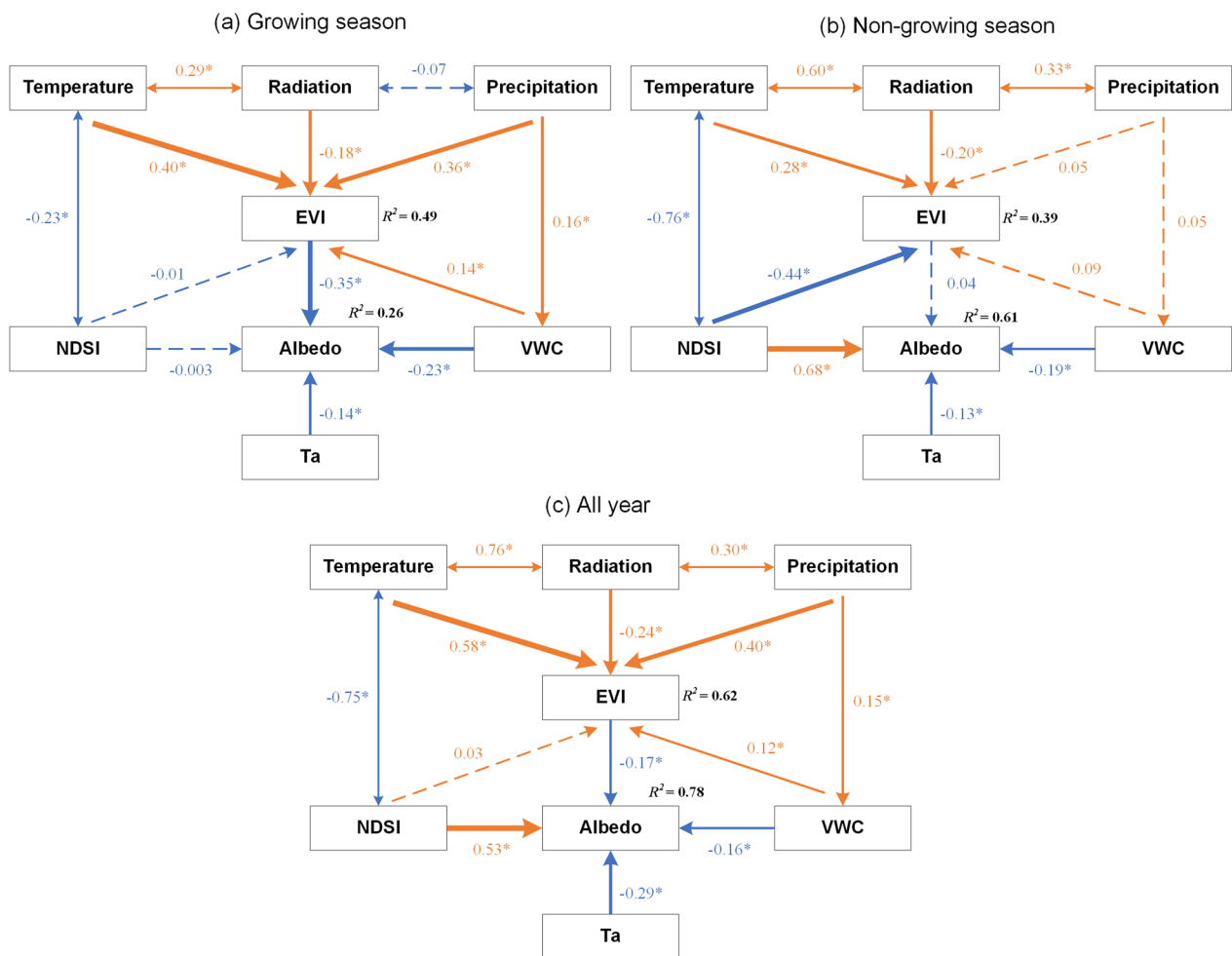


Fig. 7 Results of the structural equation models (SEMs) explaining the direct influences of the volume moisture content (VWC), enhanced vegetation index (EVI) and albedo for the growing season (a), non-growing season (b), and the whole year (c). Indirect influences of temperature, radiation, and precipitation are considered via their direct influences on the EVI, VWC, and NDSI. Significance levels are indicated by solid arrows and insignificant relationships by dashed-arrows. The numbers on each line indicate the estimated standardized path coefficient. Coefficients of determination (R^2) for explained variables are given below the variable names

had a significant positive effect (Fig. 7). The EVI showed positive control on albedo during the GS but not during the NGS as indicated by standardized path coefficients of -0.35 and 0.04 , respectively. The direct influences of VWC and T_a on albedo were significant for both seasons and at annual scale. The standardized path coefficient for VWC was -0.23 for the GS, -0.19 for the NGS, and -0.16 for the annual scale. The standardized path coefficient for the indirect effect of VWC in the GS was -0.05 (i.e. impacting albedo through its influence on the EVI). The sum of the direct and indirect effects of VWC on albedo in the GS was -0.28 . For the whole year, the standardized path coefficients for the indirect and total effects of VWC on the albedo were -0.02 and -0.18 , respectively. The standardized path coefficients of the T_a were -0.14 , -0.13 and -0.29 for the GS, NGS, and

annual scale, respectively. For annual scale, the influence of EVI and VWC were equally important while NDSI was more important, with standardized path coefficients of -0.17 , -0.16 , and 0.53 , respectively.

Relationships among other variables showed that temperature and precipitation had a strong positive control on EVI during the GS, while the effect of radiation via EVI was negative. The VWC showed a positive control on the EVI in both the GS (Additional file 1: Table S1), with standardized path coefficients of 0.14 (Fig. 7). Additionally, precipitation had a direct positive effect on VWC.

We further quantified the effects of the EVI and VWC on albedo and $GW I_{\Delta\alpha}$ at each site. The responses of albedo to the VWC and EVI ($\Delta\alpha$) varied greatly among sites with negative relationships. The regression coefficients (i.e. slopes in the regression) of albedo with

the EVI ranged from -0.411 to -0.016 while varying from -0.046 to 0.278 with the VWC. The $\text{GWI}_{\Delta\alpha}$ corresponding to the changes in EVI ranged from 0.007 to $0.186 \text{ kg CO}_2 \text{ m}^{-2} \text{ yr}^{-1}$, but varied from 0.028 to $0.122 \text{ kg CO}_2 \text{ m}^{-2} \text{ yr}^{-1}$ with VWC. The responses of albedo and $\text{GWI}_{\Delta\alpha}$ to the EVI and VWC at the four sites in Mongolia were generally higher than those in China. At the three sites in northeastern China and one site in Inner Mongolia, the response of albedo to the VWC was stronger than that to the EVI.

Discussion

The complex influences on albedo in the grasslands

In this study, we examined the interactive effects of vegetation greenness, soil moisture, climate, and snow cover on albedo in grasslands of East Asia. Temporally, both albedo and its potential drivers showed clear seasonal changes. As expected, albedo was lower in the GS than in the NGS, while vegetation grassland index (i.e. EVI) showed an opposite seasonal pattern (Fig. 2), resulting in a negative relationship (Fig. 4; Tables 2, 3). With a high EVI (i.e. high leaf area), less incoming solar radiation is reflected or scattered by the canopies, resulting in an albedo of ~ 0.20 during the growing season (Hammerle et al. 2008). However, the albedo-EVI relationship is complicated by human-induced disturbances. The albedo of the clipped site (CHA-CMDW) was not as high as expected compared to that of the fenced site (CHA-NENU) in spite of their close locations (i.e. similar snow cover, microclimate, and SZA, Fig. 2). With clipping treatments in August, the daily EVI of the two sites showed striking differences. The EVI was higher in CHA-NENU after clipping in August compared with low values in June and July (Fig. 3a), which were in agreement with in situ measurements (Dong et al. 2021). However, EVI differences alone cannot explain the differences in albedo between the two sites, as we also observed that the albedo of CHA-NENU was often higher than that of CHA-CMDW during the GS (Fig. 3c). A possible reason could be differences in soil moisture between the two sites, especially during the growing season. Soil characteristics (i.e. moisture, texture and structure) directly influence surface albedo (Ångström 1925). Albedo decreased with soil moisture (Fig. 5) because of internal reflection on the thin water film covering the soil particles and higher thermal capacity and thermal conductivity, and a darker surface can be observed when soil moisture is higher (Planet 1970; Wang et al. 2005). Human disturbances can significantly alter the soil moisture of terrestrial ecosystems. In the CHA-CMDW region, historical overgrazing has been suggested to have substantially influenced the structural and compositional aspects of grasslands, possibly leading to reductions in soil moisture (Dong et al. 2021).

This could be primarily attributed to the reduced canopy cover, or leaf area, which may limit the interception of wind-blown snow during the winter and augment heat exchange between the soil and the atmosphere (Yan et al. 2018). In addition, the trampling from livestock can compact the soil, impeding moisture capacity and transfer between the surface and the soil, potentially decreasing soil moisture (Zhao et al. 2011). In summary, our study highlighted the interplay between vegetation greenness, soil moisture, and albedo in dryland grasslands, and the impact of human disturbances on these relationships.

Snow cover and T_a are additional variables indicating changed albedo. Snow albedo is considerably higher than that of vegetation and soil, with fresh snow exhibiting reflectivity values of 0.8 – 1.0 (Chen 2021). Therefore, the seasonal dynamics of snowfall are directly related to surface albedo variations. Similarly, T_a , representing the ratio of incoming short-wave radiation to radiation at the top of the atmosphere, depends on factors such as solar angles and atmospheric conditions such as clouds and aerosols (Perez et al. 1990). For instance, T_a is low in early morning and late afternoon because of high solar zenith angle and large atmospheric optical thickness (Yang et al. 2020). At this time, short-wave radiation is more susceptible to attenuation than longwave radiation. Additionally, plants exhibit lower reflectance in the visible and near-infrared bands than in the longwave part, leading to higher albedo in early morning and late afternoon. However, T_a is also affected by cloud cover. Under such circumstances, diffuse radiation becomes a prominent part of radiation (Misson et al. 2005), leading to an insensitivity of albedo to solar zenith angle and increased energy absorption by vegetation (Gu et al. 2002). Thus, low albedo is expected compared to clear-sky conditions. The relationship between T_a and albedo depends on mechanisms operating at different temporal and in different regional contexts. In this study, we observed a negative correlation between T_a and albedo, emphasizing the importance of the relationship between T_a and solar zenith angle in semi-arid regions.

Our synthetic analysis of nine sites revealed a significant correlation between albedo and both the EVI and VWC during the GS, whereas a low correlation was found between the EVI and albedo in the NGS (Tables 2 and 3). Among sites used in this study, grasslands rapidly turn yellow during the non-growing season, exposing significant amounts of soil (Fig. 3, Chen et al. 2022a). Importantly, the VWC still exhibited higher variability in the NGS, thus retaining its significance as the exposed soil area increased (Fig. 3). A better fit by cubic models instead of linear models demonstrates that the relationship between soil moisture, greenness, and albedo can be nonlinear (Yang et al. 2020). This means that certain

regions may be more sensitive to human perturbations, resulting in stronger changes in albedo. For instance, in extremely arid conditions, albedo may respond rapidly to changes in soil moisture (Fig. 5). Overall, EVI only played a role during the growing season, while the VWC was important throughout the year. It is worth noting that the relationship between albedo and the VWC and EVI varies greatly between sites (Table 2), likely because differences in vegetation-specific hydrometeorological conditions can cause different near-infrared absorptions and reflections (Zheng et al. 2019).

The significance of soil moisture for surface albedo should not be overlooked. Our results clearly indicate that even in the growing season soil water conditions can significantly alter the surface albedo of grasslands. The relative contributions of VWC and EVI were close in both the mixed-effect models and SEMs (Additional file 1: Table S2; Fig. 7). Albedo can be considered as the joint contribution of soil albedo and canopy albedo (Sellers 1985). In semi-arid areas such as Inner Mongolia, soil albedo is generally higher than canopy albedo (Carrer et al. 2014). Some studies have reported that variations in vegetation greenness in GSs is a crucial factor to determine albedo in drylands (Tian et al. 2014; Zheng et al. 2019) because of the high sensitivity of albedo to the large differences between vegetation albedo and soil albedo. In this study, we found that soil moisture was as crucial as vegetation greenness in determining the albedo of grasslands. This can be attributed to two factors. Firstly, the sparse canopy of grasslands may result in a significant contribution of soil background to reflectance, leading to a higher overall contribution of soil albedo (Hammerle et al. 2008). Secondly, in semi-arid regions, irregular rainfall is the only source of water in soils (Sala and Lauenroth 1982), which means that soil moisture can fluctuate easily and affect soil albedo.

Implication of $\text{GWI}_{\Delta\alpha}$

We adopted a widely used method to calculate the potential contributions of variations of vegetation greenness and soil moisture in GS to annual $\text{GWI}_{\Delta\alpha}$ (Abraha et al. 2021; Bright & Lund 2021; Chen 2021; Lei et al. 2023). The contribution of growing season albedo to annual RF is greater than that of non-growing season albedo, which is consistent with previous estimates (Tian et al. 2017; Lei et al. 2023). Potential increases in EVI and VWC on grassland ecosystems produce positive $\text{GWI}_{\Delta\alpha}$ (i.e. warming effect) by lowering surface albedo. For example, a 0.1 change in the EVI and VWC could induce a 0.0008–0.0218 and 0.0024–0.0147 reduction in albedo, respectively, corresponding to a 0.007 to 0.186 and 0.028 to 0.122 $\text{kg CO}_2 \text{ m}^{-2} \text{ yr}^{-1}$ variation in $\text{GWI}_{\Delta\alpha}$ (Fig. 8).

To emphasize the importance of $\text{GWI}_{\Delta\alpha}$, we compared it to the carbon budgets of the same grasslands. Previous studies have shown that the net ecosystem productivity (NEP) of semi-arid grasslands varies greatly. The global average NEP of grasslands is about 0.36 $\text{kg CO}_2 \text{ m}^{-2} \text{ yr}^{-1}$ (Chen 2021). The four grasslands in Mongolia were carbon sources, with annual mean NEP of -0.7 to -0.21 $\text{kg CO}_2 \text{ m}^{-2} \text{ yr}^{-1}$ (Shao et al. 2017), while the grassland sites in northeastern China had an annual mean NEP of ~ 0.24 $\text{kg CO}_2 \text{ m}^{-2} \text{ yr}^{-1}$ (Dong et al. 2021). Our results suggest that $\text{GWI}_{\Delta\alpha}$ induced by fluctuations in the EVI and VWC in Mongolia reaches 0.113 $\text{kg CO}_2 \text{ m}^{-2} \text{ yr}^{-1}$, which could produce opposite climate effects if NEP were combined with $\text{GWI}_{\Delta\alpha}$. It is worth noting that $\text{GWI}_{\Delta\alpha}$ caused by variation of the EVI and VWC over time may be insignificant because albedo might return to its prior-to-disturbance level, while the climate effect of greenhouse gases works on a longer time scale (Bright and Lund. 2021; Forster et al. 2021). The magnitude of the climate impact of albedo and NEP depends on climate and geographical location. For example, Lawrence et al. (2022) reviewed the biophysical and biogeochemical impacts of global deforestation, suggesting that in mid-latitude regions ($> 50^\circ$), net climate cooling from deforestation is dominated by increased albedo, even though it results in a significant carbon debt. However, due to regional differences, the balance between NEP and albedo can vary significantly. Rohatyn et al. (2022) recently demonstrated that in some dryland regions, the conversion from grassland to forest did not lead to higher NEP but resulted in decreased albedo, while in other regions, the opposite was observed. The reasons for these differences may involve multiple factors, including climate, vegetation, and other surface characteristics. Therefore, understanding how changes in dryland ecosystems (i.e. climate change and human activities) alter surface biophysical properties is crucial for formulating effective land-based mitigation policies.

Human disturbances have produced profound impacts on arid ecosystems, especially on changes in surface properties. When coupled with climate change, their impacts may further exacerbate changes in surface attributes. For example, overgrazing in the CHA-NENU site has led to soil deterioration, affected soil water conservation capacity, caused soil salinization, and changed the microclimate (Dong et al. 2021). Through satellite-derived EVI observation we found that the grassland recovered for a decade, yet the substantial effects on albedo from reduced soil moisture and soil salinization remain irreversible. Recovery from clipping or grazing on grasslands—the two most widely practised human

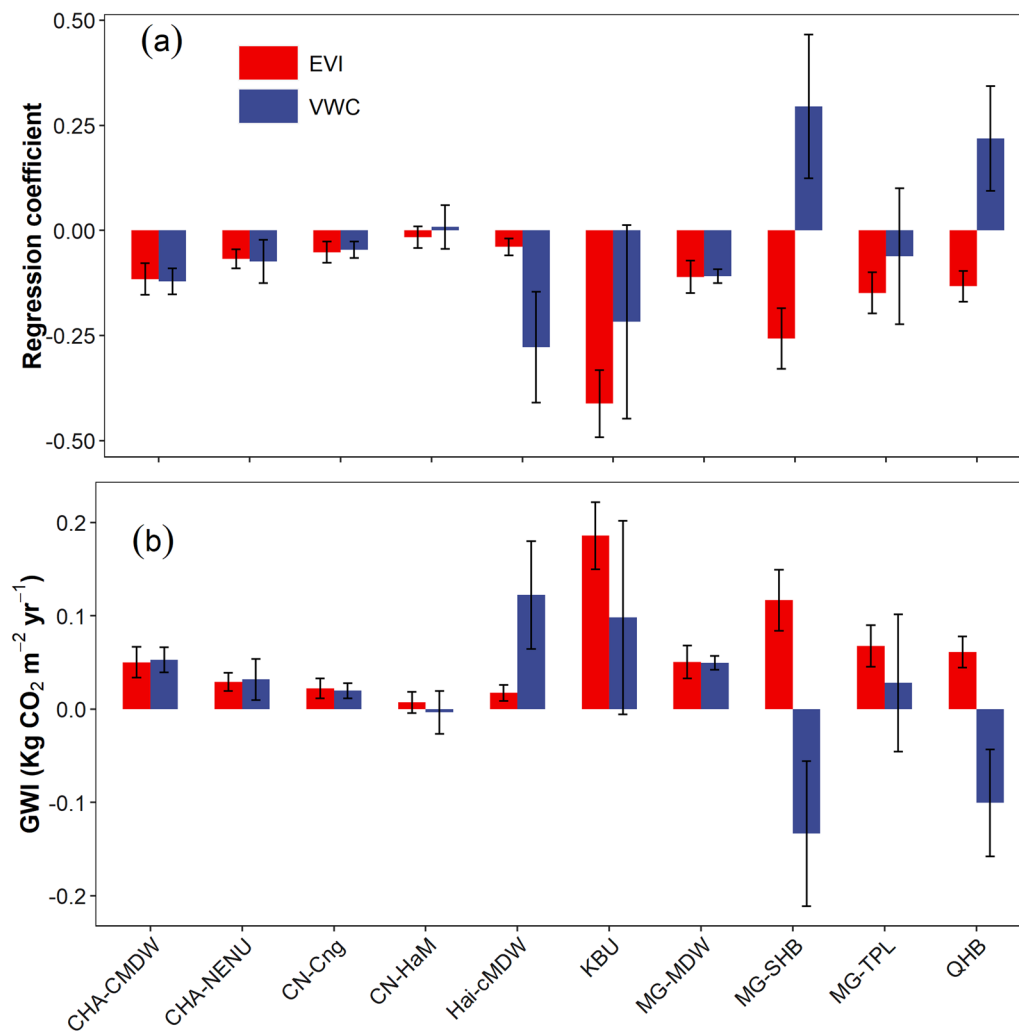


Fig. 8 Regression coefficients (i.e. slopes of the regression) for albedo vs. EVI and albedo vs. VWC and albedo-induced global warming impact ($GWI_{\Delta\alpha}$) at the ten study sites. The error bar indicates standard deviation

disturbances—can increase vegetation greenness, reduce surface albedo and have a climate impact similar to greenhouse gas emissions to some extent (Fig. 3), while reduction in soil moisture can have the opposite effect (without accounting for the influence on evapotranspiration). Clearly, our assessment of albedo-induced climate cooling should consider both positive and negative impacts.

Nonetheless, the climate cooling effects from elevated albedo following land use change (i.e. $GWI_{\Delta\alpha}$) are among the few cooling effects following intensified land use change in Asian drylands in recent decades (Forster et al. 2021). Scientific investigations of the underlying mechanisms of albedo change are clearly needed in an integrated and holistic understanding of social-environmental systems. While more research is needed to accurately quantify $GWI_{\Delta\alpha}$ and comprehend the interactions

between human societies and the environment, more direct measurements of albedo in different ecosystems and regions are needed. Our understanding of dryland ecosystems is presently constrained by uneven measurement networks across extensive spatial scales and limited data sharing. Satellite observations provide a fundamental means of monitoring large-scale surface attribute changes. However, their effectiveness is hindered by differences in frequency and spatial resolution (Smith et al. 2019). For example, optical remote sensing data provide only snapshots of the surface (e.g., vegetation indices) due to cloud and bad weather, while microwave remote sensing data typically have coarse spatial resolution (e.g., soil moisture observations). Moreover, it is essential to integrate remote sensing and in situ measurements to gain a detailed understanding of complex processes, which will allow to develop better parameterization for earth system

models and comprehend the non-linear carbon cycle and albedo dynamics in the future.

In this study, we combined satellite and flux tower observations. However, we acknowledge that there may be some scale mismatch between satellite and in situ observations (Additional file 1: Figs. S1, S2), which may affect the relationship between the EVI and albedo (Chu et al. 2021). Shadow effects resulting from the complex composition and structure of vegetation communities may induce uncertainty on reflectance of grassland (Alavipanah et al. 2022). However, dynamics of EVI and NEP correspond well in our sites and shadow effects may be relatively small in grassland ecosystems because of the relative low canopy height and leaf area. We only discussed the relationship between the surface VWC, EVI, NDSI, T_a , and albedo, while deep-layer VWC, snow days, phenology, and weather conditions may also have an impact on albedo (Yang et al. 2020). In addition, our data cover a short period of time while other factors such as the VWC and EVI may vary at longer time scales. Finally, the mechanisms affecting albedo need to be explored at different time scales and in combination with more systematic observations in future studies.

Conclusions

We explored the changes in albedo of grasslands in the context of intensified human activities in a dryland region of East Asia and analysed the complex interactions among the albedo, EVI, VWC, T_a , and NDSI. We found that: (a) the EVI and VWC exerted significant effects on albedo changes during the growing season, while the VWC also indirectly influenced albedo by affecting the EVI; the relative contributions of these variables were similar in the growing season; (b) the VWC and NDSI were the dominant factors in the non-growing season; and (c) growing season albedo dominated the variations of $\text{GWI}_{\Delta\alpha}$ through changing in EVI and VWC. By analysing multi-year ground observations in five grassland ecosystems in drylands Eastern Asia, we highlighted the complex interactions among vegetation, soil moisture, and albedo, in which anthropogenic disturbances play non-negligible roles. Therefore, in the context of rapidly changing socio-environmental systems in drylands, understanding the synergy between multiple factors, including albedo, is essential to understand the role of these ecosystems in a changing climate.

Abbreviations

EVI	Enhanced vegetation index
VWC	Surface soil volumetric water content
NDSI	Normalized Difference Snow Index
T_a	Clearness index
RF	Radiative forcing

GWI	Global warming potential
$\text{GWI}_{\Delta\alpha}$	Albedo-induced global warming potential

Supplementary Information

The online version contains supplementary material available at <https://doi.org/10.1186/s13717-024-00493-w>.

Additional file 1: Figure S1. Land cover of study sites and nearby areas. The centre of the figure shows the location of the study sites, and the circles around the centre are buffer zones with radii of 250 m, 500 m, 1000 m, 1500 m, and 2000 m, respectively. **Figure S2.** Enhanced Vegetation Index (EVI) of study sites and nearby areas. The centre of the figure shows the location of the study sites, and the circles around the centre are buffer zones with radii of 250 m, 500 m, 1000 m, 1500 m, and 2000 m, respectively. **Table S1.** Summary of linear regression between enhanced vegetation index (EVI) and soil volumetric water content (VWC) for ten grass sites in this study. **Table S2.** Summary of linear mixed-effect model for the monthly albedo, VWC, T_a , NDSI and EVI.

Acknowledgements

This research was supported by the National Key Research and Development Program of China.

Author contributions

JC, XL and QZ developed the ideas for this manuscript. QZ conducted the model runs and data analysis, and drafted the manuscript. All authors contributed to the writing and revision of the manuscript.

Funding

This work was funded by the National Key Research and Development Program of China (2022YFC3703304 and 2022YFC3703301).

Availability of data and materials

The data in site CN-CNG can be downloaded from <https://fluxnet.org/>; data in site KBU and QHB can be downloaded from <http://asiaflux.net/>; other data used and/or analysed during the current study are available from the corresponding author on reasonable request.

Declarations

Ethics approval and consent to participate

Not applicable.

Consent for publication

Not applicable.

Competing interests

The authors declare that they have no competing interests.

Received: 21 October 2023 Accepted: 8 February 2024

Published online: 04 March 2024

References

- Abraha M, Chen J, Hamilton SK et al (2021) Albedo-induced global warming impact of Conservation Reserve Program grasslands converted to annual and perennial bioenergy crops. *Environ Res Lett* 16(8):084059
- Alavipanah SK, Karimi FM, Sedighi A et al (2022) The shadow effect on surface biophysical variables derived from remote sensing: a review. *Land* 11(11):2025
- Ångström A (1925) The albedo of various surfaces of ground. *Geogr Ann* 7(4):323–342
- Betts RA (2000) Offset of the potential carbon sink from boreal forestation by decreases in surface albedo. *Nature* 408(6809):187–190

- Briegleb BP, Minnis P, Ramanathan V, Harrison E (1986) Comparison of regional clear-sky albedos inferred from satellite observations and model computations. *J Appl Meteorol Clim* 25(2):214–226
- Bright RM, Lund MT (2021) CO₂-equivalence metrics for surface albedo change based on the radiative forcing concept: a critical review. *Atmos Chem Phys* 21(12):9887–9907
- Bright RM, O'Halloran TL (2019) Developing a monthly radiative kernel for surface albedo change from satellite climatologies of Earth's shortwave radiation budget: CACK v1.0. *Geosci Model Dev* 12(9):3975–3990
- Carrer D, Meurey C, Ceamanos X, Roujean J-L, Calvet J-C, Liu S (2014) Dynamic mapping of snow-free vegetation and bare soil albedos at global 1 km scale from 10-year analysis of MODIS satellite products. *Remote Sens Environ* 140:420–432
- Carrer D, Pique G, Ferlicoq M, Ceamanos X, Ceschia E (2018) What is the potential of cropland albedo management in the fight against global warming? A case study based on the use of cover crops. *Environ Res Lett* 13(4):044030
- Chen J (2021) *Biophysical models and applications in ecosystem analysis*. Michigan State University Press, Michigan
- Chen J, John R, Sun G et al (2018) Prospects for the sustainability of social-ecological systems (SES) on the Mongolian plateau: five critical issues. *Environ Res Lett* 13(12):123004
- Chen J, Dong G, Chen J et al (2022a) Ecosystem balance and partitioning over grasslands on the Mongolian Plateau. *Ecol Indic* 135:108560
- Chen J, John R, Yuan J et al (2022b) Sustainability challenges for the social-environmental systems across the Asian Drylands Belt. *Environ Res Lett* 17(2):023001
- Chu H, Luo X, Ouyang Z et al (2021) Representativeness of eddy-covariance flux footprints for areas surrounding AmeriFlux sites. *Agric For Meteorol* 301–302:108350
- Coll J, Li X (2018) Comprehensive accuracy assessment of MODIS daily snow cover products and gap filling methods. *ISPRS J Photogramm* 144:435–452
- Cui X, Niu H, Wu J et al (2006) Response of chlorophyll fluorescence to dynamic light in three alpine species differing in plant architecture. *Environ Exp Bot* 58(1):149–157
- Dedieu JP, Lessard-Fontaine A, Ravazzani G, Cremonese E, Shalpykova G, Beniston M (2014) Shifting mountain snow patterns in a changing climate from remote sensing retrieval. *Sci Total Environ* 493:1267–1279
- Dong G, Zhao F, Chen J et al (2021) Land uses changed the dynamics and controls of carbon-water exchanges in alkali-saline Songnen Plain of Northeast China. *Ecol Indic* 133:108353
- Fan Y, Chen J, Shirkey G et al (2016) Applications of structural equation modeling (SEM) in ecological studies: an updated review. *Ecol Process* 5:19
- Fick SE, Hijmans RJ (2017) WorldClim 2: new 1-km spatial resolution climate surfaces for global land areas. *Int J Climatol* 37(12):4302–4315
- Forster P, Storelvmo T, Armour K et al (2021) The Earth's energy budget, climate feedbacks, and climate sensitivity. In: Masson-Delmotte V, Zhai P, Pirani A et al (eds), *Climate change 2021: the physical science basis*. Contribution of Working Group I to the Sixth Assessment Report of the Intergovernmental Panel on Climate Change. Cambridge University Press, Cambridge, United Kingdom and New York, NY, USA, pp 923–1054
- Groisman PY, Clark EA, Kattsov VM et al (2009) The Northern Eurasia Earth Science Partnership: an example of science applied to societal needs. *Bull Am Meteorol Soc* 90(5):671–688
- Gu L, Baldocchi D, Verma SB et al (2002) Advantages of diffuse radiation for terrestrial ecosystem productivity. *J Geophys Res-Atmos* 107(D5-6):4050
- Hammerle A, Haslwanter A, Tappeiner U, Cernusca A, Wohlfahrt G (2008) Leaf area controls on energy partitioning of a temperate mountain grassland. *Biogeosciences* 5(2):421–431
- Huete A, Didan K, Miura T, Rodriguez EP, Gao X, Ferreira LG (2002) Overview of the radiometric and biophysical performance of the MODIS vegetation indices. *Remote Sens Environ* 83(1):195–213
- John R, Chen J, Lu N, Wilske B (2009) Land cover/land use change in semi-arid Inner Mongolia: 1992–2004. *Environ Res Lett* 4(4):045010
- John R, Chen J, Kim Y et al (2016) Differentiating anthropogenic modification and precipitation-driven change on vegetation productivity on the Mongolian Plateau. *Landsc Ecol* 31(3):547–566
- Kato T, Tang Y, Gu S et al (2006) Temperature and biomass influences on inter-annual changes in CO₂ exchange in an alpine meadow on the Qinghai-Tibetan Plateau. *Glob Change Biol* 12(7):1285–1298
- Kawamura K, Akiyama T, Yokota H et al (2005) Monitoring of forage conditions with MODIS imagery in the Xilingol steppe, Inner Mongolia. *Int J Remote Sens* 26(7):1423–1436
- Kuznetsova A, Brockhoff PB, Christensen RHB (2017) lmerTest package: tests in linear mixed effects models. *J Stat Softw* 82(13):1–26
- Lawrence D, Coe M, Walker W, Verchot L, Vandecar K (2022) The unseen effects of deforestation: biophysical effects on climate. *Front For Glob Change* 5:756115
- Lee X, Goulden ML, Hollinger DY et al (2011) Observed increase in local cooling effect of deforestation at higher latitudes. *Nature* 479(7373):384–387
- Lei C, Chen J, Robertson GP (2023) Climate cooling benefits of cellulosic bioenergy crops from elevated albedo. *GCB Bioenergy* 15:1373–1386. <https://doi.org/10.1111/gcbb.13098>
- Li SG, Asanuma J, Eugster W et al (2005) Net ecosystem carbon dioxide exchange over grazed steppe in central Mongolia. *Glob Change Biol* 11(11):1941–1955
- Li Z, Yang J, Gao X et al (2019) The relationship between surface spectral albedo and soil moisture in an arid Gobi area. *Theor Appl Climatol* 136(3):1475–1482
- Lobell DB, Asner GP (2002) Moisture effects on soil reflectance. *Soil Sci Soc Am J* 66(3):722–727
- Misson L, Lunden M, McKay M, Goldstein AH (2005) Atmospheric aerosol light scattering and surface wetness influence the diurnal pattern of net ecosystem exchange in a semi-arid ponderosa pine plantation. *Agric For Meteorol* 129(1):69–83
- Myneni RB, Williams DL (1994) On the relationship between FAPAR and NDVI. *Remote Sens Environ* 49(3):200–211
- Ouyang Z, Sciusco P, Jiao T et al (2022) Albedo changes caused by future urbanization contribute to global warming. *Nat Commun* 13(1):3800
- Perez R, Ineichen P, Seals R, Zelenka A (1990) Making full use of the clearness index for parameterizing hourly insolation conditions. *Sol Energy* 45(2):111–114
- Planet WG (1970) Some comments on reflectance measurements of wet soils. *Remote Sens Environ* 1(2):127–129
- Qi J, Xin X, John R, Groisman P, Chen J (2017) Understanding livestock production and sustainability of grassland ecosystems in the Asian Dryland Belt. *Ecol Process* 6:22
- Riggs GA, Hall DK, Román MO (2017) Overview of NASA's MODIS and Visible Infrared Imaging Radiometer Suite (VIIRS) snow-cover Earth System Data Records. *Earth Syst Sci Data* 9(2):765–777
- Rohatyn S, Yakir D, Rotenberg E, Carmel Y (2022) Limited climate change mitigation potential through forestation of the vast dryland regions. *Science* 377(6613):1436–1439
- Sala OE, Lauenroth WK (1982) Small rainfall events: an ecological role in semi-arid regions. *Oecologia* 53(3):301–304
- Sciusco P, Chen J, Abraha M et al (2020) Spatiotemporal variations of albedo in managed agricultural landscapes: inferences to global warming impacts (GWI). *Landsc Ecol* 35(6):1385–1402
- Sciusco P, Chen J, Giannico V et al (2022) Albedo-induced global warming impact at multiple temporal scales within an upper midwest USA watershed. *Land* 11(2):283
- Sellers PJ (1985) Canopy reflectance, photosynthesis and transpiration. *Int J Remote Sens* 6(8):1335–1372
- Shao C, Chen J, Chu H et al (2017) Grassland productivity and carbon sequestration in Mongolian grasslands: the underlying mechanisms and nomadic implications. *Environ Res* 159:124–134
- Smith WK, Dannenberg MP, Yan D et al (2019) Remote sensing of dryland ecosystem structure and function: progress, challenges, and opportunities. *Remote Sens Environ* 233:111401
- Tian L, Zhang Y, Zhu J (2014) Decreased surface albedo driven by denser vegetation on the Tibetan Plateau. *Environ Res Lett* 9(10):104001
- Tian L, Chen J, Zhang Y (2017) Growing season carries stronger contributions to albedo dynamics on the Tibetan plateau. *PLoS ONE* 12(9):e0180559
- Venkatesh K, John R, Chen J et al (2022a) Untangling the impacts of socio-economic and climatic changes on vegetation greenness and productivity in Kazakhstan. *Environ Res Lett* 17(9):095007
- Venkatesh K, John R, Chen J et al (2022b) Optimal ranges of social-environmental drivers and their impacts on vegetation dynamics in Kazakhstan. *Sci Total Environ* 847:157562
- Wang K, Wang P, Liu J, Sparrow M, Haginoya S, Zhou X (2005) Variation of surface albedo and soil thermal parameters with soil moisture content at

- a semi-desert site on the western Tibetan Plateau. *Bound-Lay Meteorol* 116(1):117–129
- Yan Y, Yan R, Chen J et al (2018) Grazing modulates soil temperature and moisture in a Eurasian steppe. *Agric For Meteorol* 262:157–165
- Yang L, Wei W, Chen L, Chen W, Wang J (2014) Response of temporal variation of soil moisture to vegetation restoration in semi-arid Loess Plateau, China. *Catena* 115:123–133
- Yang J, Li Z, Zhai P, Zhao Y, Gao X (2020) The influence of soil moisture and solar altitude on surface spectral albedo in arid area. *Environ Res Lett* 15(3):035010
- Yuan J, Chen J, Sciusco P et al (2022) Land use hotspots of the two largest landlocked countries: Kazakhstan and Mongolia. *Remote Sens* 14(8):1805
- Zhang Y, Wang X, Hu R, Pan Y, Zhang H (2014) Variation of albedo to soil moisture for sand dunes and biological soil crusts in arid desert ecosystems. *Environ Earth Sci* 71(3):1281–1288
- Zhang H, Zhang F, Zhang G et al (2019) Ground-based evaluation of MODIS snow cover product V6 across China: implications for the selection of NDSI threshold. *Sci Total Environ* 651:2712–2726
- Zhao Y, Peth S, Reszkowska A et al (2011) Response of soil moisture and temperature to grazing intensity in a *Leymus chinensis* steppe, Inner Mongolia. *Plant Soil* 340(1):89–102
- Zheng L, Zhao G, Dong J et al (2019) Spatial, temporal, and spectral variations in albedo due to vegetation changes in China's grasslands. *ISPRS J Photogramm* 152:1–12

Publisher's Note

Springer Nature remains neutral with regard to jurisdictional claims in published maps and institutional affiliations.